

Analyze of the interfacial stress in reinforced concrete beams strengthened with externally bonded CFRP plate

Lazreg Hadji ^{*1}, T. Hassaine Daouadji ^{1,2},
M. Ait Amar Meziane ^{1,2} and E.A. Adda Bedia ²

¹ Université Ibn Khaldoun, BP 78 Zaaroura, 14000 Tiaret, Algérie

² Laboratoire des Matériaux & Hydrologie, Université de Sidi Bel Abbes, 22000 Sidi Bel Abbes, Algérie

(Received February 27, 2015, Revised March 29, 2015, Accepted November 03, 2015)

Abstract. A theoretical method to predict the interfacial stresses in the adhesive layer of reinforced concrete beams strengthened with externally bonded carbon fiber-reinforced polymer (CFRP) plate is presented. The analysis provides efficient calculations for both shear and normal interfacial stresses in reinforced concrete beams strengthened with composite plates, and accounts for various effects of Poisson's ratio and Young's modulus of adhesive. Such interfacial stresses play a fundamental role in the mechanics of plated beams, because they can produce a sudden and premature failure. The analysis is based on equilibrium and deformations compatibility approach developed by Tounsi. In the present theoretical analysis, the adherend shear deformations are taken into account by assuming a parabolic shear stress through the thickness of both the reinforced concrete beam and bonded plate. The paper is concluded with a summary and recommendations for the design of the strengthened beam.

Keywords: FRP composites; interfacial stresses; reinforced concrete beam; strengthening; adhesive

1. Introduction

Advanced composite materials, e.g., fiber – reinforced polymers (FRP), have found their new applications in the rehabilitation of reinforced concrete structure (Triantafillou 1998, Quantrill and Hollaway 1998). Compared with the traditional materials, composite materials have some unique features, i.e., high strength and stiffness to weight ratio, attractive corrosion resistance and ease of handling and application (Meier *et al.* 1993, Meier 1997). Among these materials, carbon fiber polymers (CFRP) are extensively used because of their unparalleled characteristics (Meier 1995, Mouring 2001). The transferring of stresses from concrete to the FRP reinforcement is central to the reinforcement effect of FRP – strengthened concrete structures. This is because the stresses are susceptible to cause the undesirable premature and brittle failure, such as debonding of the soffit plate from the RC beam. This debonding failure mode is brittle and prevents the full utilization of the tensile strength of the bonded plate. It is therefore important to understand the mechanism of this debonding failure mode and develop sound design rules. This brittle mode of failure is a result of the high shear and vertical normal (peeling) stress concentrations arising at the edges of the bonded FRP strip. Hence, this limited area in the close vicinity of the bonded strip edge, subjected

*Corresponding author, Ph.D., E-mail: had_laz@yahoo.fr

to high peeling and interfacial shear stresses, proves to be among the most critical parts of the strengthened beam. Consequently, the determination of interfacial stresses has been researched for the last decade for beams bonded with either steel or advanced composite materials. In particular, several closed – form analytical solutions have been developed (Vilnay 1988, Smith and Teng 2001). All these solutions are for linear elastic materials and employ the same key assumption that the adhesive is subject to normal and shear stresses that are constant across the thickness of the adhesive layer. It is this key assumption that enables relatively simple closed – form solutions to be obtained. In the existing solutions, two different approaches have been employed. Smith and Teng (2001) considered directly deformation compatibility conditions.

The advantages of the FRP retrofitting method and performances of the hybrid structure involve the excellent properties of the FRP composite. The FRP composite is of high stiffness and strength, low weight, corrosion resistance, and electromagnetic neutrality. The retrofitting process of the existing structures becomes quick and simple due to the lower weight. The performance enhancement of such hybrid structures, however, depends on properties of the interface between the steel beam and FRP. The present research focuses on the influence of adhesive properties on the interfacial stress in externally FRP plated reinforced concrete beams. The behaviour of the interface between the reinforced concrete beam and FRP can influence the performance of hybrid beam and is influenced by many factors such as the properties and geometries of the steel beam, FRP and adhesive layer. The interface transfers the stresses from reinforced concrete to FRP plate. Therefore, a comprehensive understanding on the stress state and the stress – transfer mechanism of the interface is necessary for the design and application of the hybrid structures. The interfacial stress of the hybrid beam has been studied by experimental and theoretical methods. The experimental technologies were applied to test the interfacial stresses (Etman and Beeby 2000, Jones *et al.* 1988). However, the experimental test of interfacial stress fields seems to be difficult because of the complicated distribution of local stresses. The analytical studies (Tounsi 2006, Tounsi *et al.* 2008) tend to develop a closed – form solutions for the interfacial shear and normal stresses. Recently Attari *et al.* (2012) investigated the flexural strengthening of concrete beams using CFRP, GFRP and hybrid FRP sheets. Xiang (Xiang and Wang 2013) presented a calculation of Flexural Strengthening of Fire-damaged reinforced concrete beams with CFRP Sheets. Zhang and Teng (2013) investigated the interaction forces in RC beams strengthened with near-surface mounted rectangular bars and strips.

Ameur *et al.* (2011) presented the finite element analysis of interfacial stresses in steel beams strengthened with a bonded hygrothermal aged CFRP plate. Boucif *et al.* (2014) presented the effect of shear deformation on interfacial stress analysis in plated beams under arbitrary loading. Krouer *et al.* (2013) studied the Fibers orientation optimization for concrete beam strengthened with a CFRP bonded plate: A coupled analytical–numerical investigation.

In this paper, the influence of the characteristics of structural adhesives on the interfacial stresses in FRP plated reinforced concrete beams is investigated theoretically. These investigations are carried out by means of a new analytical method which takes into account the adherend shear deformations. The importance of including shear – lag effect of the adherends was shown firstly by Tsai *et al.* (1998) in adhesive lap joints. Tounsi (2006) has extended this theory to study concrete beam strengthened by FRP plate. The basic assumption in these two studies is a linear distribution of shear stress across the thickness of the adherends. However, it is well known that in beam theory, this distribution is parabolic through the depth of beam. In the present developed method this later assumption is taken into consideration. The methods predicts stress distributions along the adhesive joint and can be used to analyze failure of the adhesive, or the substrates in the

immediate vicinity of the joint, failure modes typically observed in adhesive joints involving metallic or FRP substrates.

2. Methods of analysing adhesive joints

Bonded joints have been used since the 1930s, but it is only relatively recently that this technology has been transferred to the construction industry. Adhesive joints in construction are often on a larger scale than those in the automotive or aerospace industries (for example), and behave in different ways. Furthermore, construction projects are one – offs and it is not economic to base design on test results, unlike other industries with long production runs. Consequently, it is important to have realistic models for the adhesive joint strength. Two approaches can be used to predict the failure of adhesive joints: a stress analysis, or a fracture mechanics approach. Fracture mechanics examines the energy required for unstable crack propagation along the joint; however, this approach has yet to be successfully applied to infrastructure strengthening applications (Buyukozturk *et al.* 2003).

After the adhesive has cured, the strengthening plate and beam act compositely, with load transferred between them by a combination of shear stresses (parallel to the joint) and peel stresses (normal to the joint). A stress analysis can be used to predict the distributions of shear and peel stress along the strengthened beam, for comparison to the limiting strength of the adhesive joint. Several closed – form stress analyses are available that predict the distribution of bond stresses along a plate bonded to a beam, for example, see (Tounsi 2006, Etman and Beeby 2000). These all assume that the adhesive is linear – elastic, but involve a variety of simplifying assumptions.

The motivation behind the approach presented in this paper was the lack of guidance for designing FRP strengthening bonded to metallic structures. The reliability of structural adhesive joint depends on several factors. Among these factors, the adhesive characteristics play an important role in the integrity and reliability of hybrid structure.

3. Methods of analysing adhesive joints

A differential section dx , can be cut out from the FRP reinforced concrete beam (Fig. 1), as shown in Fig. 2. The composite beam is made from three materials: reinforced concrete beam, adhesive layer and FRP reinforcement. In the present analysis, linear elastic behaviour is regarded to be for all the materials; the adhesive is assumed to play a role only in transferring the stresses from the concrete to the FRP reinforcement and the stresses in the adhesive layer do not change through the direction of the thickness.

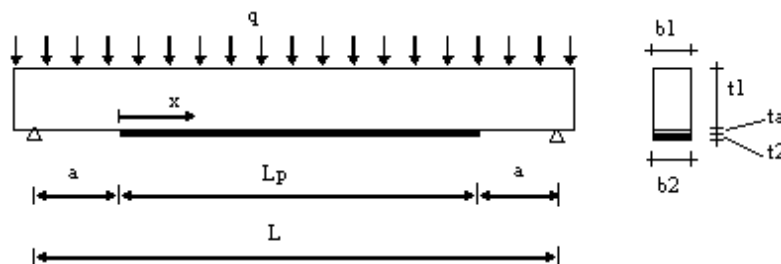


Fig. 1 Simply supported beam strengthened with bonded composite plate

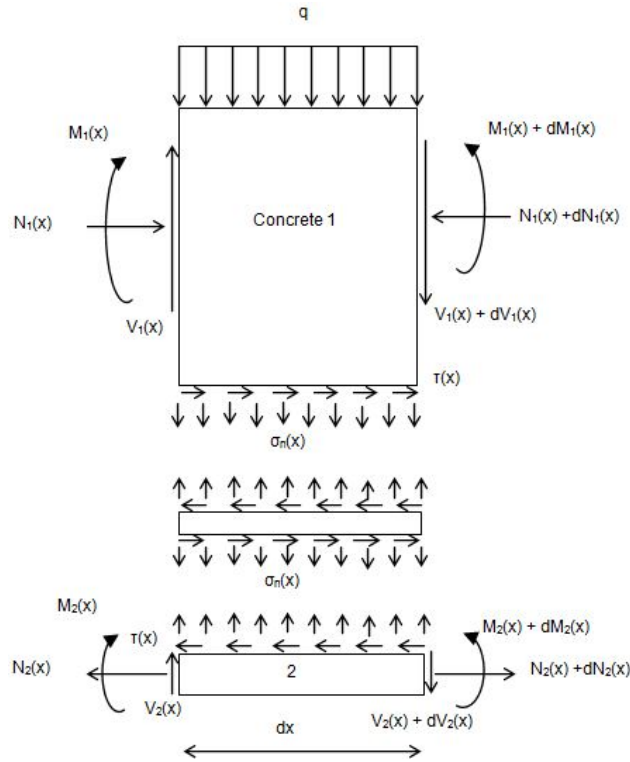


Fig. 2 Simply Forces in infinitesimal element of a soffit – plated beam

3.1 Basic equation of elasticity

The strains in the reinforced concrete beam near the adhesive interface can be expressed as

$$\epsilon_1(x) = \frac{du_1(x)}{dx} = \epsilon_1^M(x) + \epsilon_1^N(x) \tag{1}$$

Where $u_1(x)$ is the longitudinal displacement at the base of reinforced concrete beam. $\epsilon_1^M(x)$ is the strain induced by the bending moment at the adherend 1 and it is written as follow

$$\epsilon_1^M(x) = \frac{y_1}{E_1 I_1} M_1(x) \tag{2}$$

Where $M_1(x)$ is the bending moment applied in the steel beam; E_1 is Young’s moduli of the reinforced concrete beam; I_1 is the second moment area; y_1 is the distance from the bottom of adherend 1 to its centroid.

$\epsilon_1^N(x)$ is the unknown longitudinal strain of the reinforced concrete beam, at the adhesive interface and it is due to the longitudinal forces. This strain is given as follow

$$\epsilon_1^N(x) = \frac{du_1^N(x)}{dx} \tag{3}$$

Where u_1^N represents the longitudinal force – induced adhesive displacement at the interface between the steel beam and the adhesive.

To determine the unknown longitudinal strain $\varepsilon_1^N(x)$ shear deformations of the reinforced concrete beam is incorporated in this analysis. It is reasonable to assume that the shear stresses, which develop in the adhesive, are continuous across the adhesive – adherend interface. In addition, equilibrium requires the shear stress be zero at the free surface. Using the same methodology developed by Tounsi (2006), this effect is taken into account. A cubic variation of longitudinal displacement $U_1^N(x, y)$ through the thickness of adherend 1 is assumed

$$U_1^N(x, y) = A_1(x)y^3 + B_1(x)y + C_1(x) \tag{4}$$

Where y is a local coordinate system with the origin at the top surface of the upper adherend Fig. 2.

The shear stresses in adherend 1 is given by

$$\sigma_{xy(1)} = G_1\gamma_{xy(1)} \tag{5}$$

With

$$\gamma_{xy(1)} = \frac{\partial U_1^N}{\partial y} + \frac{\partial W_1^N}{\partial x} \tag{6}$$

G_1 is the transverse shear modulus of the adherend 1. Neglecting the variations of transverse displacement W_1^N (induced by the longitudinal forces) with the longitudinal coordinate x .

$$\gamma_{xy(1)} \approx \frac{\partial U_1^N}{\partial y} \tag{7}$$

And the shear stresses are expressed as

$$\sigma_{xy(1)} = G_1(3A(x)y^2 + B(x)) \tag{8}$$

The shear stresses must satisfy the following conditions

$$\sigma_{xy(1)}(x, t_1) = \tau(x) = \tau_a \tag{9}$$

$$\sigma_{xy(1)}(x, 0) = 0 \tag{10}$$

t_1 is the thickness of adherend 1.

Condition (9) follows from continuity and assumption of the uniform shear stresses ($\tau(x) = \tau_a$) through the thickness of adhesive. Condition (10) states there is no shear stresses at the top surface of the adherend 1 (i.e., at $y = 0$). These conditions yield

$$\sigma_{xy(1)} = \frac{\tau_a}{t_1^2} y^2 \tag{11}$$

Then with a linear material constitutive relationship the adherend shear strain γ_1 for the adherend 1 is written as

$$\gamma_{xy(1)} = \gamma_1 = \frac{\tau_a}{G_1 t_1^2} y^2 \quad (12)$$

The longitudinal displacement functions U_1^N for the upper adherend, due to the longitudinal forces, is given as

$$U_1^N(y) = U_1^N(0) + \int_0^y \gamma_1(y) dy = U_1^N(0) + \frac{\tau_a}{3G_1 t_1^2} y^3 \quad (13)$$

Where $U_1^N(0)$ represents the displacement at the top surface of the upper adherend (due to the longitudinal forces).

Note that due to the perfect bonding of the joints, the displacements are continuous at the interfaces between the adhesive and adherends. As a result, the u_1^N (the adhesive displacement at the interface between the adhesive and upper adherend) should be the same as the upper adherend displacement at the interface. Based on Eq. (13) the u_1^N can be expressed as

$$u_1^N = U_1^N(y = t_1) = U_1^N(0) + \frac{\tau_a t_1}{3G_1} \quad (14)$$

Using Eq. (14), Eq. (13) can be rewritten as

$$U_1^N(y) = u_1^N + \frac{\tau_a}{3G_1 t_1^2} y^3 - \frac{\tau_a t_1}{3G_1} \quad (15)$$

The longitudinal resultant force, N_1 for the upper adherend, is

$$N_1 = b_1 \int_0^{t_0} \sigma_1^N(y) dy + b_0 \int_{t_0}^{t_1-t_0} \sigma_1^N(y) dy + b_1 \int_{t_1-t_0}^{t_1} \sigma_1^N(y) dy \quad (16)$$

With $b_0 = b_1$ width of the concrete beam and $t_0 = t_1$ height of the concrete beam.

Where σ_1^N is longitudinal normal stress for the upper adherend. By changing these stresses into functions of displacements and substituting Eq. (15) into the displacement, Eq. (16) can be rewritten as

$$N_1 = E_1 b_1 \int_0^{t_0} \frac{dU_1^N}{dx} dy + E_1 b_0 \int_{t_0}^{t_1-t_0} \frac{dU_1^N}{dx} dy + E_1 b_1 \int_{t_1-t_0}^{t_1} \frac{dU_1^N}{dx} dy \quad (17)$$

Hence, the longitudinal strains induced by the longitudinal forces Eq. (3) can be expressed as

$$\varepsilon_1^N(x) = \frac{du_1^N}{dx} = \frac{N_1}{E_1 A_1} + \frac{1}{12G_1 t_1^2 A_1} \left(b_1 \left[-t_0^4 - t_1^4 + (t_1 - t_0)^4 + 8t_1^3 t_0 \right] + b_0 \left[4t_1^3 (t_1 - 2t_0) - (t_1 - t_0)^4 + t_0^4 \right] \right) \frac{d\tau(x)}{dx} \quad (18)$$

Substituting Eqs. (18) and (2) into Eqs. (1), this latter becomes

$$\begin{aligned} \varepsilon_1(x) &= \frac{du_1(x)}{dx} \\ &= \frac{y_1}{E_1 I_1} M_1(x) + \frac{N_1(x)}{E_1 A_1} + \frac{1}{12 G_1 t_1^2 A_1} \left[b_1 \left(-t_0^4 - t_1^4 + (t_1 - t_0)^4 + 8t_1^3 t_0 \right) \right. \\ &\quad \left. + b_0 \left(4t_1^3 (t_1 - 2t_0) - (t_1 - t_0)^4 + t_0^4 \right) \right] \frac{d\tau(x)}{dx} \end{aligned} \quad (19)$$

Where $N(x)$ are the axial forces in each adherend, A_1 the cross – sectional area.

Since the composite laminate is an orthotropic material, its material properties vary from layer to layer. In current study, the laminate theory is used to determine the stress and strain behaviours of the externally bonded composite plate in order to investigate the whole mechanical performance of the composite – strengthened structure. The effective moduli of the composite laminate are varied by the orientation of the fibre directions and arrangements of the laminate patterns. The laminate theory is used to estimate the strain of the symmetrical composite plate (Herakovich, 1998), i.e.

$$\varepsilon_x^0 = A'_{11} N_x \frac{1}{b_2} \quad \text{and} \quad k_x = D'_{11} M_x \frac{1}{b_2} \quad (20)$$

$[A'] = [A^{-1}]$ is the inverse of the extensional matrix $[A]$; $[D'] = [D^{-1}]$ is the inverse of the flexural matrix; b_2 is a width of FRP plate.

Using CLT, the strain at the top of the FRP plate 2 is given as

$$\varepsilon_2(x) = \varepsilon_x^0 - k_x \frac{t_2}{2} \quad (21)$$

Substituting Eq. (20) in (21) gives the following equation

$$\varepsilon_2(x) = \frac{du_2(x)}{dx} = -D'_{11} \frac{t_2}{2b_2} M_2(x) + A'_{11} \frac{N_2(x)}{b_2} \quad (22)$$

Where

$$N_2(x) = N_x \quad \text{and} \quad M_2(x) = M_x \quad (23)$$

$M(x)$, $N(x)$ and $V(x)$ are the bending moment, axial and shear forces in the adherend.

By adopting the equilibrium conditions of the reinforced concrete beam, we have

$$\text{Along } x \text{ – direction:} \quad N_2(x) = N_x \quad \text{and} \quad M_2(x) = M_x \quad (24)$$

Where $\tau(x)$ is shear stress in the adhesive layer.

$$\text{Along } y \text{ – direction:} \quad \frac{dV_1(x)}{dx} = -[\sigma_n(x)b_2 + q] \quad (25)$$

Where $V_1(x)$ is shear force applied in the reinforced concrete beam; $\sigma_n(x)$ is normal stress in the adhesive layer and q is the uniformly distributed load.

$$\text{Moment equilibrium: } \frac{dM_1(x)}{dx} = V_1(x) - \tau(x)b_2y_1 \quad (26)$$

The equilibrium of the external FRP reinforcement along x -, y - direction and moment equilibrium can be also written as

$$\text{Along } x \text{ - direction: } \frac{dN_2(x)}{dx} = \tau(x)b_2 \quad (27)$$

$$\text{Along } y \text{ - direction: } \frac{dV_2(x)}{dx} = \sigma_n(x)b_2 \quad (28)$$

$$\text{Moment equilibrium: } \frac{dM_2(x)}{dx} = V_2(x) - \tau(x)b_2 \frac{t_2}{2} \quad (29)$$

Where $V_2(x)$ is shear force applied in the external FRP reinforcement.

3.2 Shear stress distribution along the FRP – beam interface

Here, it is considered that the bending stiffness of the external FRP reinforcement is far less than of the beam to be strengthened and the bending moment in the external FRP reinforcement can be neglected for simplicity in the derivation of shear stress.

The shear stress in the adhesive can be expressed as follows

$$\tau(x) = K_s \Delta u(x) = K_s [u_2(x) - u_1(x)] \quad (30)$$

Where K_s is shear stiffness of the adhesive per unit length and can be deduced as

$$K_s = \frac{\tau(x)}{\Delta u(x)} = \frac{\tau(x)}{\Delta u(x)/t_a} \frac{1}{t_a} = \frac{G_a}{t_a} \quad (31)$$

$\Delta u(x)$ is relative horizontal displacement at the adhesive interface; G_a is the shear modulus in the adhesive and t_a is the thickness of the adhesive.

Substituting Eqs. (19) and (22) into Eq. (30) and differentiating the resulting equation once yields

$$\frac{d\tau(x)}{dx} = K_s \left[\frac{-y_2}{b_2} D'_{11} M_2(x) + \frac{A'_{11}}{b_2} N_2(x) - \frac{y_1}{E_1 I_1} M_1(x) - \frac{N_1(x)}{E_1 A_1} - \frac{1}{12G_1 t_1^2 A_1} \left(b_1 \left[-t_0^4 - t_1^4 + (t_1 - t_0)^4 + 8t_1^3 t_0 \right] + b_0 \left[4t_1^3 (t_1 - 2t_0) - (t_1 - t_0)^4 + t_0^4 \right] \right) \frac{d\tau(x)}{dx} \right] \quad (32)$$

Assuming equal curvature in the beam and the FRP plate, the relationship between the moments in the two adherends can be expressed as

$$M_1(x) = R M_2(x) \quad (33)$$

With

$$R = \frac{E_1 I_1 D'_{11}}{b_2} \quad (34)$$

Moment equilibrium of the differential segment of the plated beam in Fig. 2 gives

$$M_T(x) = M_1(x) + M_2(x) + N(x)[y_1 + y_2 + t_a] \quad (35)$$

Where, $M_T(x)$ is the total applied moment and from Eqs. (24) and (27), the axial forces are given as

$$N_1(x) = -N(x) = -b_2 \int_0^x \tau(x) \quad \text{and} \quad N_2(x) = N(x) = b_2 \int_0^x \tau(x) \quad (36)$$

The bending moment in each adherend, expressed as a function of the total applied moment and the interfacial shear stress, is given as

$$M_1(x) = \frac{R}{R+1} \left[M_T(x) - b_2 \int_0^x \tau(x)(y_1 + y_2 + t_a) dx \right] \quad (37)$$

and

$$M_2(x) = \frac{1}{R+1} \left[M_T(x) - b_2 \int_0^x \tau(x)(y_1 + y_2 + t_a) dx \right] \quad (38)$$

The first derivative of the bending moment in each adherend gives

$$\frac{dM_1(x)}{dx} = \frac{R}{R+1} [V_T(x) - b_2 \tau(x)(y_1 + y_2 + t_a)] \quad (39)$$

and

$$\frac{dM_2(x)}{dx} = \frac{1}{R+1} [V_T(x) - b_2 \tau(x)(y_1 + y_2 + t_a)] \quad (40)$$

Differentiating Eq. (32)

$$\begin{aligned} \frac{d^2 \tau(x)}{dx^2} = K_S \left(\frac{A'_{11}}{b_2} \frac{dN_2(x)}{dx} - \frac{y_2}{b_2} D'_{11} \frac{dM_2(x)}{dx} - \frac{y_1}{E_1 I_1} \frac{dM_1(x)}{dx} - \frac{1}{E_1 A_1} \frac{dN_1(x)}{dx} \right) - \\ \frac{K_S}{12 G_1 t_1^2 A_1} \left[b_1 \left((t_1 - t_0)^4 - t_0^4 - t_1^4 + 8 t_1^3 t_0 \right) + b_0 \left(4 t_1^3 (t_1 - 2 t_0) - (t_1 - t_0)^4 + t_0^4 \right) \right] \frac{d^2 \tau(x)}{dx^2} \end{aligned} \quad (41)$$

Substitution of the shear forces (Eqs. (39) and (40)) and axial forces Eq. (36) into Eq. (41) gives the following governing differential equation for the interfacial shear stress.

$$\frac{d^2 \tau(x)}{dx^2} - K_1 b_2 \left(\frac{(y_1 + y_2)(y_1 + y_2 + t_a)}{E_1 I_1 D'_{11} + b_2} + A'_{11} + \frac{b_2}{E_1 A_1} \right) \tau(x) + K_1 \left(\frac{(y_1 + y_2) D'_{11}}{E_1 I_1 D'_{11} + b_2} \right) V_T(x) = 0 \quad (42)$$

$$K_1 = \frac{1}{\left(\frac{t_a}{G_a} + \frac{t_1}{4G_1}\xi\right)} \quad (43)$$

and ξ is a geometrical coefficient which is given as

$$\xi = \frac{1}{3A_1t_1^3} \left[b_1(-t_0^4 - t_1^4 + (t_1 - t_0)^4 + 8t_0t_1^3) + b_0(4t_1^3(t_1 - 2t_0) - (t_1 - t_0)^4 + t_0^4) \right] \quad (44)$$

For a rectangular section ($b_1 = b_0$), $\xi = 1$, however, for I – beam section (the present case) we have $\xi < 1$.

For simplicity, the general solutions presented below are limited to loading which is either concentrated or uniformly distributed over part or the whole span of the beam, or both. For such loading, $d_2VT(x)/dx_2 = 0$, and the general solution to Eq. (42) is given by

$$\tau(x) = B_1 \cosh(\lambda x) + B_2 \sinh(\lambda x) + m_1 V_T(x) \quad (45)$$

Where

$$\lambda^2 = K_1 b_2 \left(\frac{(y_1 + y_2)(y_1 + y_2 + t_a)}{E_1 I_1 D'_{11} + b_2} + A'_{11} + \frac{b_2}{E_1 A_1} \right) \quad (46)$$

and

$$m_1 = \frac{K_1}{\lambda^2} \left(\frac{(y_1 + y_2) D'_{11}}{E_1 I_1 D'_{11} + b_2} \right) \quad (47)$$

B_1 and B_2 are constant coefficients determined from the boundary conditions.

In the present study, a simply supported beam is investigated which is subjected to a uniformly distributed load.

Considering the boundary conditions:

- (1) Due to symmetry, the shear stress at mid – span is zero, i.e.

$$\tau\left(\frac{L_P}{2}\right) = B_1 \cosh\left(\lambda \frac{L_P}{2}\right) + B_2 \sinh\left(\lambda \frac{L_P}{2}\right) + m_1 V_T\left(\frac{L_P}{2}\right) = 0 \quad (48)$$

Where L_P is the length of the FRP plate (see Fig. 1).

- (2) At the end of the FRP plate, the longitudinal force [$N_1(0) = N_2(0)$] and the moment $M_2(0)$ are zero. As a result, the moment in the section at the plate curtailment is resisted by the beam alone and can be expressed as

$$M_1(0) = M_T(0) = \frac{qa}{2}(L - a) \quad (49)$$

Applying the above boundary condition in Eq. (30)

$$\frac{d\tau(x=0)}{dx} = -m_2 M_T(0) \quad \text{with} \quad m_2 = \frac{K_1 y_1}{E_1 I_1} \quad (50)$$

From the above three equations

$$B_2 = \frac{-m_2qa}{2\lambda}(L-a) + \frac{m_1}{\lambda}q \tag{51}$$

$$B_1 = -B_2 \tanh\left(\frac{\lambda L_p}{2}\right); \quad V_T\left(\frac{L_p}{2}\right) = 0 \tag{52}$$

For practical cases $\frac{\lambda L_p}{2} > 10$ and as a result $\tanh\left(\frac{\lambda L_p}{2}\right) \approx 1$. So the expression for B_1 can be simplified to

$$B_1 = -B_2 \tag{53}$$

Substitution of B_1 and B_2 into Eq. (45) gives an expression for the interfacial shear stress at any point

$$\tau(x) = \left(\frac{m_2a}{2}(L-a) - m_1\right) \frac{qe^{-\lambda x}}{\lambda} + m_1q\left(\frac{L}{2} - a - x\right) \tag{54}$$

$$0 \leq x \leq L_p$$

Where q is the uniformly distributed load and x , a , L and L_p are defined in Fig. 1.

In the case where the beam is subjected to a two symmetric point loads, the general solution for the interfacial shear stress is given by the following expressions Tounsi (2006)

$a < b$

$$\tau(x) = \begin{cases} \frac{m_2}{\lambda}Pae^{-\lambda x} + m_1P \cosh(\lambda\lambda x)^{-k} & 0 \leq x \leq (b-a) \\ \frac{m_2}{\lambda}Pae^{-\lambda x} + m_1P \sinh(k)e^{-\lambda x} & (b-a) \leq x \leq \frac{L_p}{2} \end{cases} \tag{55}$$

$a > b$

$$\tau(x) = \frac{m_2}{\lambda}Pbe^{-\lambda x} \quad 0 \leq x \leq L_p \tag{56}$$

Where P is the concentrated load and $k = \lambda(b - a)$. The expression of m_1 and m_2 takes into considerations the shear deformation of adherends.

4.1 Comparison of analytical solutions

A comparison of the interfacial shear and normal stresses from the different existing closed – form solutions and the present new solution is undertaken in this section. An undamaged RC beam bonded with a CFRP soffit plate is considered. The beam is simply supported and subjected to a uniformly distributed load. A summary of the geometric and material properties is given in Table 1. The span of The RC beam is 3000 mm, the distance from the support to the end of the plate is 300 mm and the uniformly distributed load is 50 KN/m.

Table 1 Dimensions and material properties

Material	E_{11} (GPa)	E_{22} (GPa)	G_{12} (GPa)	ν_{12}	Width (mm)	Depth (mm)
CFRP plate	140	10	5	0.28	$b_2 = 200$	$t_2 = 4$
RC beam	30	30		0.18	$b_1 = 200$	$t_1 = 300$
Adhesive layer	3	3	1.08	0.35	$b_2 = 200$	$t_a = 4$

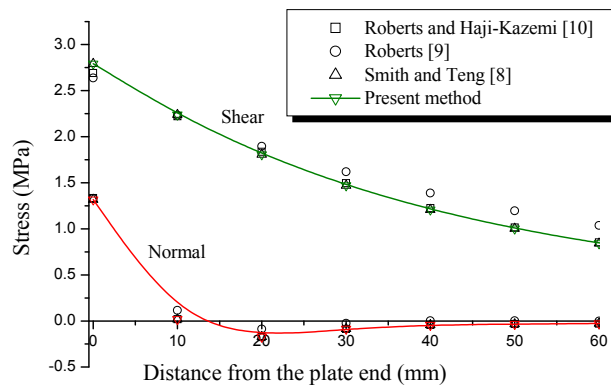


Fig. 3 Comparison of interfacial shear and normal stresses for an RC beam with a bonded CFRP plate subjected to a uniformly distributed load

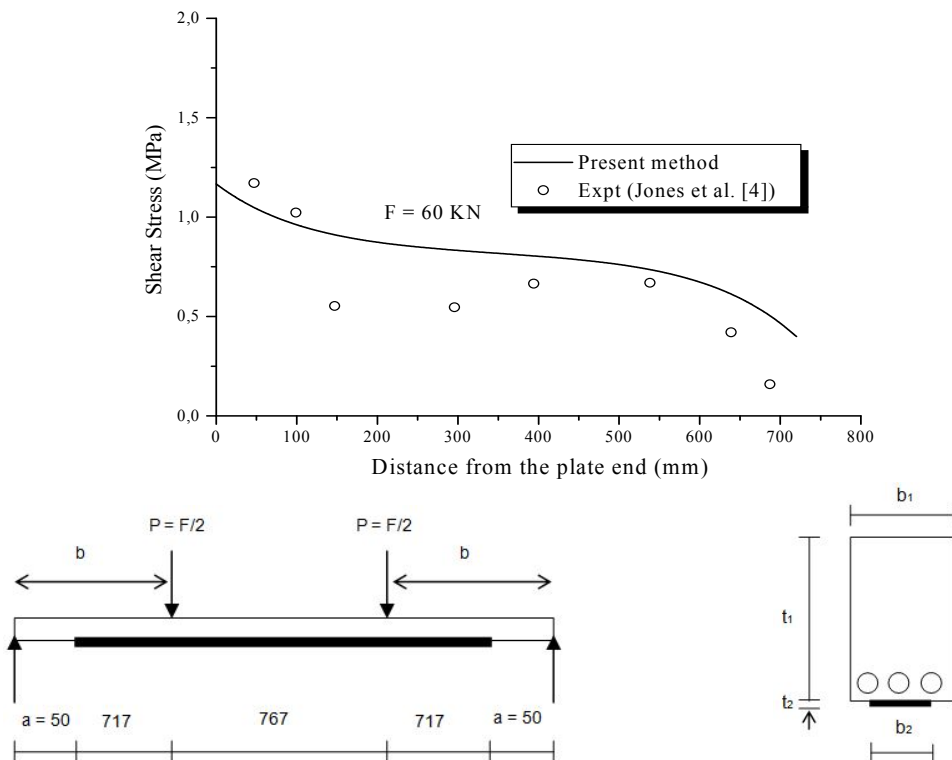


Fig. 4 Comparison of interfacial shear stress of the steel plated RC beam with the experimental results from Jones *et al.* (1988)

Fig. 3 plots the interfacial shear and normal stresses near the plate end for the example RC beam bonded with a CFRP plate for the uniformly distributed load case. Overall, the predictions of the different solutions agree closely with each other. The interfacial normal stress is seen to change sign at a short distance away from the plate end.

4.2 Comparison with experimental results

To validate the present method, a rectangular section ($\zeta = 1$) is used here. One of the tested beams bonded with reinforced concrete plate by Jones *et al.* (1988), beams F31, is analyzed here using the present improved solution. The beam is simply supported and subjected to four – point bending, each at the third point. The geometry and materials properties of the specimen are summarized in Table 1.

The interfacial shear stress distributions in the beam bonded with a soffit steel plate under the applied load 60 kN, i.e., $P = 30$ kN in Fig. 4, are compared between the experimental results and those obtained by the present method. As it can be seen from Fig. 3, the comparison shows encouraging agreement with the experimental results.

4. Results and discussion

For each of the five Poisson’s ratios of the adhesives, results for edge stresses, corresponding to various Young’s modulus of adhesive E_a , ranging between 0.001 and 30 GPa are presented in graphical forms.

4.1 Effect of Young’s modulus:

The two edge stresses (shear and normal stress) corresponding to Poisson’s ratio $\nu_a = 0.3$ are shown in Fig. 5. From Fig. 5, it is seen that both shear and normal interfacial stress increase gradually as the Young’s modulus of adhesive increase from 0.001 to 30 GPa.

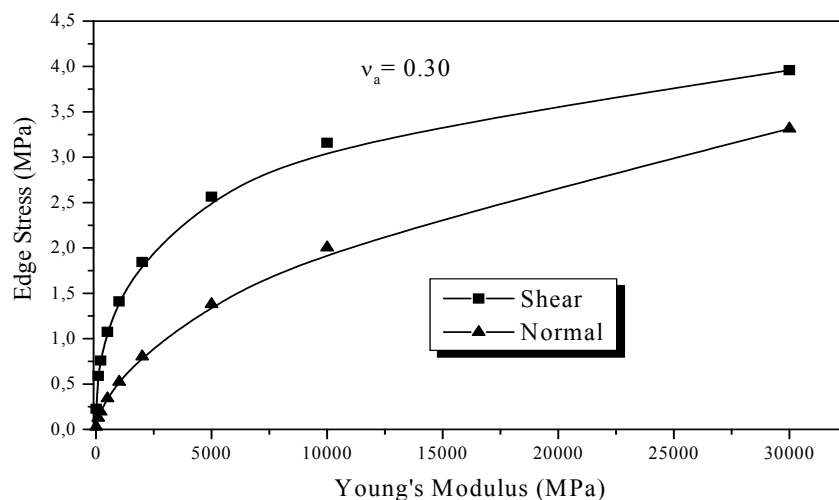


Fig. 5 Interfacial maximum stress versus Young’s modulus of adhesive for Poisson’ ratio $\nu_a = 0.3$

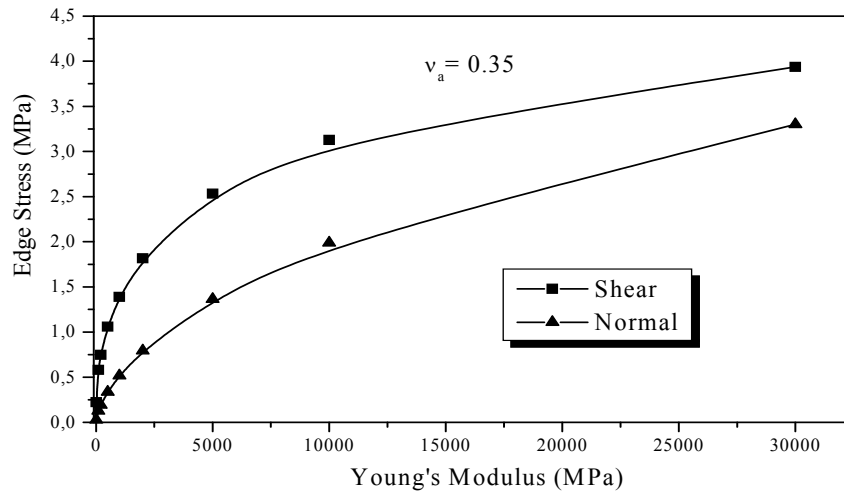


Fig. 6 Interfacial maximum stress versus Young's modulus of adhesive for Poisson's ratio $\nu_a = 0.35$

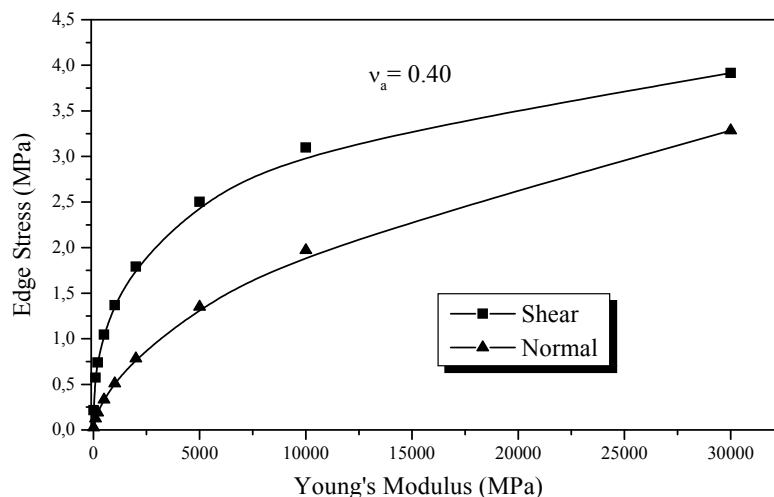


Fig. 7 Interfacial maximum stress versus Young's modulus of adhesive for Poisson's ratio $\nu_a = 0.40$

Figs. 6 to 9 show that when Poisson's ratio $\nu_a = 0.35, 0.4, 0.45$ and 0.5 , similar variations of the maximum interfacial stress with Young's modulus as in the case of $\nu_a = 0.3$ (Fig. 5) are obtained. The interfacial stresses shown in Fig. 5 for Poisson's ratio $\nu_a = 0.3$ and Young's modulus, E_a , greater than 5 GPa are representative of those that will be obtained when very hard adhesives such as ceramic glue are used. Similarly, the interfacial stresses shown in Figs. 6 and 7 for Poisson's ratios $\nu_a = 0.35$ and 0.4 and for Young's modulus, E_a , within the range $0.05 - 5$ GPa apply to adhesives comprising of multiple part epoxies. On the other hand, the interfacial stresses shown in figure 8 and 9 for Poisson's ratios $\nu_a = 0.45$ and 0.5 and for Young's modulus, E_a , less than 0.05 GPa are representative of those manifested by rubber - like or elastomeric adhesives.

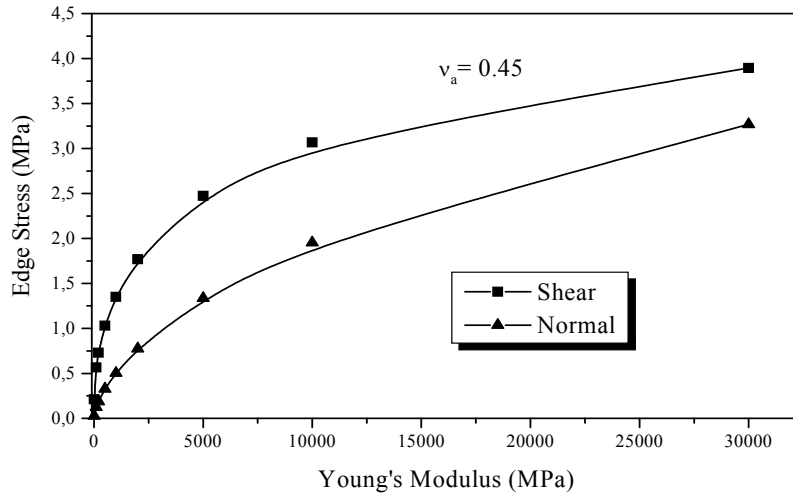


Fig. 8 Interfacial maximum stress versus Young's modulus of adhesive for Poisson's ratio $v_a = 0.45$

5.2 Effect of Poisson's ratio

The two maximum adhesive stresses (shear and normal stress) versus Poisson's ratio of adhesive for different value of Young's modulus of adhesive ($Ea = 1, 2, 5, 10$ and 30 GPa) are shown in Fig. 10. It can be seen from the presented results that the Poisson's ratio of adhesive has almost no effect on the variation of the maximum adhesive stresses. However, these stresses increase gradually with the Young's modulus of adhesive. We note that the adhesives with Young's modulus smaller than 1 GPa are not commonly used in practice. In addition, the adhesives with Young's modulus $Ea = 30$ GPa is used only for theoretical comparison.

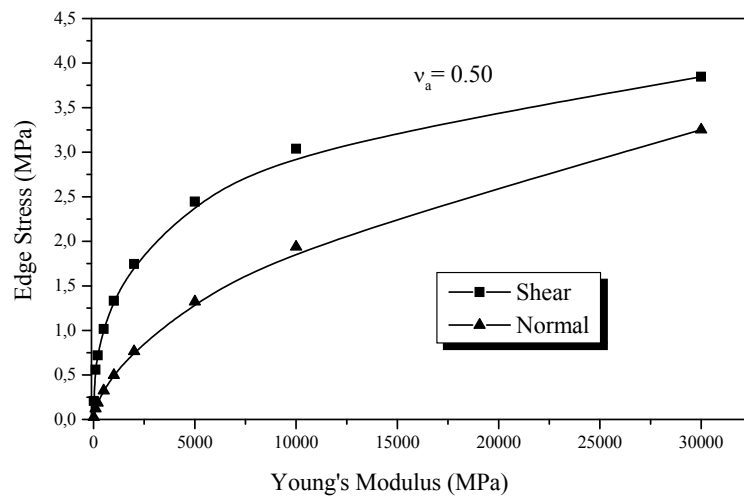


Fig. 9 Interfacial maximum stress versus Young's modulus of adhesive for Poisson's ratio $v_a = 0.50$

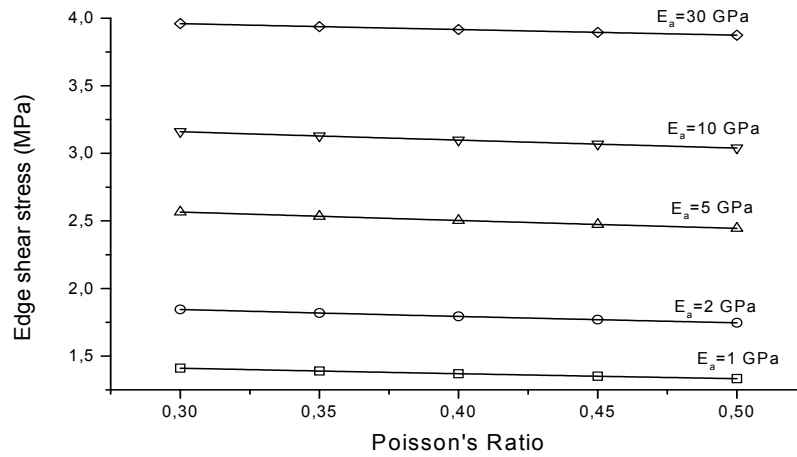


Fig. 10 Interfacial maximum shear stress versus Poisson's ratio of adhesive

5. Conclusions

The influence of adhesive properties on the adhesive stresses in beams strengthened with FRP plates has been investigated using an improved analytical model. The adherend shear deformations are taken into account by assuming a parabolic shear stress through the thickness of both the reinforced concrete beam and bonded plate. By comparing with experimental results, the present closed – solution provides satisfactory predictions to the interfacial shear stress in the plated beams. The maximum interfacial stresses have been analysed using adhesives of various Young's modulus and Poisson's ratio properties. In general, the maximum interfacial stress increase with an increase in the Young's modulus of adhesive, but does not appear to change significantly with an increase in the Poisson's ratio.

Acknowledgments

The authors thank the referees for their valuable comments.

References

- Ameur, M., Daouadji, T.H., Abbes, B., Tounsi, A. and Adda, E.A. (2011), "Finite element analysis of interfacial stresses in steel beams strengthened with a bonded hygrothermal aged CFRP plate", *Revue des composites et des matériaux avancés*, **21**(2), 193-207.
- Attari, N., Amziane, S. and Chemrouk, M. (2012), "Flexural strengthening of concrete beams using CFRP, GFRP and hybrid FRP sheets", *Construct. Build. Mater.*, **37**, 746-757.
- Boucif, G., Tounsi, A. and Adda Bedia, E.A. (2014), "The effect of shear deformation on interfacial stress analysis in plated beams under arbitrary loading", *Int. J. Adhes. Adhes.*, **48**, 1-13.
- Buyukozturk, O., Gunes, O. and Karaca, E. (2003), "Progress on understanding debonding problems in reinforced concrete and steel members strengthened using FRP composites", *Construct. Build. Mater.*, **18**, 9-19.
- Etman, E.E. and Beeby, A.W. (2000), "Experimental program and analytical study of bond stress distributions on a composite plate bonded to a reinforced RC beam", *Cement Concrete Compos.*, **22**(4),

281-291.

- Guenaneche, B., Tounsi, A. and Adda Bedia, E.A. (2014), "Effect of shear deformation on interfacial stress analysis in plated beams under arbitrary loading", *Int. J. Adhes. Adhes.*, **48**, 1-13.
- Herakovich, C.T. (1998), "Mechanics of fibrous composites", *John Wiley & Sons, Inc.*
- Jones, R., Swamy, R.N. and Charif, A. (1988), "Plate separation and anchorage of reinforced concrete beams strengthened by epoxy – bonded steel plates", *The Struct. Engr.*, **66**(5/1), 85-94.
- Krou, B., Bernard, F. and Tounsi, A. (2013), "Fibers orientation optimization for concrete beam strengthened with a CFRP bonded plate: A coupled analytical–numerical investigation", *Eng. Struct.*, **56**, 218-227.
- Meier, U. (1995), "Strengthening of structures using carbon fiber/epoxy composites", *Construct. Build. Mater.*, **9**(6), 341-351.
- Meier, U. (1997), "Post strengthening by continuous fiber laminates in Europe", *Proceedings of the 3rd International Symposium on Non-metallic (FRP) Reinforcement for Concrete Structures*, Japan Concrete Institute, Sapporo, Japan, month, pp. 42-56.
- Meier, U., Deuring, M., Meier, H. and Schwegler, G. (1993), "Strengthening of structures with advanced composites", *Alternative Materials for the Reinforcement and Prestressing of Concrete*, (J.L. Clarke editor), Glasgow, Scotland, pp. 153-171.
- Mouring, S.E., Barton, J.R.O. and Simmons, D.K. (2001), "Reinforced concrete beams externally retrofitted with advanced composites", *Adv. Compos. Mater.*, **10**(2-3), 139-146.
- Quantrill, R.J. and Hollaway, L.C. (1998), "The flexural rehabilitation of reinforced concrete beams by the use of prestressed advanced composite plates", *Compos. Sci. Technol.*, **58**(8), 1259-1275.
- Smith, S.T. and Teng, J.G. (2001), "Interfacial stresses in plated RC beams", *Eng. Struct.*, **23**(7), 857-871.
- Tounsi, A. (2006), "Improved theoretical solution for interfacial stresses in concrete beams strengthened with FRP plate", *Int. J. Solid. Struct.*, **43**(14-15), 4154-4174.
- Tounsi, A., Hassaine Daouadji, T., Benyoucef, S. and Adda, E.A. (2008), "Interfacial stresses in FRP-plated RC beams: Effect of adherend shear deformations", *Int. J. Adhes. Adhes.*, **29**(4), 343-351.
- Triantafillou, T.C. (1998), "A new possibility for the shear strengthening of concrete, masonry and wood", *Compos. Sci. Technol.*, **58**(8), 1285-1295.
- Tsai, M.Y., Oplinger, D.W. and Morton, J. (1998), "Improved theoretical solutions for adhesive lap joints", *Int. J. Solid. Struct.*, **35**(12), 1163-1185.
- Vilnay, O. (1988), "The analysis of reinforced concrete beams strengthened by epoxy bonded steel plates", *Int. J. Cement Compos. Lightweight Concrete*, **10**(2), 73-78.
- Xiang, K. and Wang, G.H. (2013), "Calculation of flexural strengthening of fire-damaged reinforced concrete beams with CFRP sheets", *Procedia Eng.*, **52**, 446-452.
- Zhang, S.S. and Teng, J.G. (2013), "Interaction forces in RC beams strengthened with near-surface mounted rectangular bars and strips", *Composites: Part B*, **45**(1), 697-709.